

HSAB Principle Applied to the Time Evolution of Chemical Reactions[†]

Pratim Kumar Chattaraj* and Buddhadev Maiti

Contribution from the Department of Chemistry, Indian Institute of Technology,
Kharagpur 721302, India

Received July 9, 2002; E-mail: pkc@chem.iitkgp.ernet.in

Abstract: Time evolution of various reactivity parameters such as electronegativity, hardness, and polarizability associated with a collision process between a proton and an X^- atom/ion ($X = \text{He}, \text{Li}^+, \text{Be}^{2+}, \text{B}^{3+}, \text{C}^{4+}$) in its ground (^1S) and excited ($^1\text{P}, ^1\text{D}, ^1\text{F}$) electronic states as well as various complexions of a two-state ensemble is studied using time-dependent and excited-state density functional theory. This collision process may be considered to be a model mimicking the actual chemical reaction between an X -atom/ion and a proton to give rise to an XH^+ molecule. A favorable dynamical process is characterized by maximum hardness and minimum polarizability values according to the dynamical variants of the principles of maximum hardness and minimum polarizability. An electronic excitation or an increase in the excited-state contribution in a two-state ensemble makes the system softer and more polarizable, and the proton, being a hard acid, gradually prefers less to interact with X as has been discerned through the drop in maximum hardness value and the increase in the minimum polarizability value when the actual chemical process occurs. Among the noble gas elements, Xe is the most reactive. During the reaction: $\text{H}_2 + \text{H}^+ \rightarrow \text{H}_3^+$ hardness maximizes and polarizability minimizes and H_2 is more reactive in its excited state. Regioselectivity of proton attack in the O-site of CO is clearly delineated wherein HOC^+ may eventually rearrange itself to go to the thermodynamically more stable HCO^+ .

Introduction

Pearson^{1–3} introduced the concept of hardness through his famous hard–soft acid–base (HSAB) principle which states that,^{1–4} “hard acids prefer to coordinate with hard bases and soft acids prefer to coordinate with soft bases for both their thermodynamic and kinetic properties”. Another important related hardness principle also proposed by Pearson⁵ is the maximum hardness principle (MHP)^{1,6,7} which states that,⁶ “there seems to be a rule of nature that molecules arrange themselves so as to be as hard as possible”. The validity of HSAB principle has been shown⁸ to somehow demand that of the MHP. Owing to the inverse relationship⁹ between hardness and polarizability a minimum polarizability principle (MPP)¹⁰

has been proposed which states that, “the natural direction of evolution of any system is toward a state of minimum polarizability”.

Density functional theory (DFT)^{3,11} has been quite successful in providing solid theoretical footing for the qualitative popular indices of chemical reactivity like electronegativity and hardness. Electronegativity (χ)¹² and hardness (η)⁴ are respectively defined for an N -electron system with energy E , as the following first and second-order derivatives

$$\chi = -\mu = -\left(\frac{\partial E}{\partial N}\right)_{v(r)} \quad (1)$$

and

$$\eta = \frac{1}{2}\left(\frac{\partial^2 E}{\partial N^2}\right)_{v(r)} = \frac{1}{2}\left(\frac{\partial \mu}{\partial N}\right)_{v(r)} \quad (2)$$

where μ and $v(r)$ are chemical potential (Lagrange multiplier associated with normalization constraint of DFT) and external potential, respectively. Equivalently, hardness can be expressed

[†] Dedicated to Professor Walter Kohn, the father of the Density Functional Theory, on his 80th birthday.

- (1) Pearson, R. G. *Chemical Hardness: Application from Molecules to Solid*; Wiley-VCH: Weinheim, 1997.
- (2) Sen, K. D.; Mingos, D. M. P. *Chemical Hardness: Structure and Bonding*; Springer: Berlin, 1993; Vol. 80.
- (3) Parr, R. G.; Yang, W. *Density Functional Theory of Atoms and Molecules*; Oxford University Press: Oxford, 1989.
- (4) Pearson, R. G. *Hard and Soft Acids and Bases*; Dowden, Hutchinson & Ross: Stroudsburg, PA, 1973. (b) Parr, R. G.; Pearson, R. G. *J. Am. Chem. Soc.* **1983**, *105*, 7512.
- (5) Pearson, R. G. *J. Chem. Edu.* **1987**, *64*, 561. Pearson, R. G. *Acc. Chem. Res.* **1993**, *26*, 250.
- (6) (a) Parr, R. G.; Chattaraj, P. K. *J. Am. Chem. Soc.* **1991**, *113*, 1854. (b) Chattaraj, P. K.; Liu, G. H.; Parr, R. G. *Chem. Phys. Lett.* **1995**, *237*, 171. (c) Ayers, P. W.; Parr, R. G. *J. Am. Chem. Soc.* **2000**, *122*, 2010.
- (7) Chattaraj, P. K. *Proc. Ind. Natl. Sci. Acad. Part. A* **1996**, *62*, 513.
- (8) (a) Chattaraj, P. K.; Lee, H.; Parr, R. G. *J. Am. Chem. Soc.* **1991**, *113*, 1855. (b) Chattaraj, P. K.; Schleyer, P. v. R. *J. Am. Chem. Soc.* **1994**, *116*, 1067. (c) Cedillo, A.; Chattaraj, P. K.; Parr, R. G. *Int. J. Quantum Chem. M. Zerner Spl. Issue* **2000**, *77*, 403.

- (9) (a) Pearson, R. G. in 2. (b) Politzer, P. *J. Chem. Phys.* **1987**, *86*, 1072. (c) Ghanty, T. K.; Ghosh, S. K. *J. Phys. Chem.* **1993**, *97*, 4951. (d) Fuentealba, P.; Reyes, O. *J. Mol. Struct. (THEOCHEM)* **1993**, *282*, 65. (e) Fuentealba, P.; Simon-Manso, Y. *J. Phys. Chem. A* **1998**, *102*, 2029.
- (10) (a) Chattaraj, P. K.; Sengupta, S. *J. Phys. Chem.* **1996**, *100*, 16 126. (b) Ghanty, T. K.; Ghosh, S. K. *J. Phys. Chem.* **1996**, *100*, 12 295.
- (11) (a) Hohenberg, P.; Kohn, W. *Phys. Rev. B* **1964**, *136*, 864. (b) Kohn, W.; Sham, L. J. *Phys. Rev. A* **1965**, *140*, 1133.
- (12) Parr, R. G.; Donnelly, D. A.; Levy, M.; Palke, W. E. *J. Chem. Phys.* **1978**, *68*, 3801.

as¹³

$$\eta = \frac{1}{N} \int \int \eta(r, r') f(r') \rho(r) dr dr' \quad (3)$$

where $f(r)$ is the Fukui function¹⁴ and the hardness kernel is given by

$$\eta(r, r') = \frac{1}{2} \frac{\delta^2 F[\rho]}{\delta \rho(r) \delta \rho(r')} \quad (4)$$

in terms of the Hohenberg–Kohn–Sham universal functional of DFT.¹¹ The wave function of an N -particle system is completely characterized by N and $\nu(r)$. Although χ and η measure the response of the system when N changes at fixed $\nu(r)$, polarizability (α) plays the same role for varying $\nu(r)$ at constant N .

So far the studies on HSAB principle has been restricted to ground states and for time-independent situations. In the present work, we analyze this principle in the light of the principles of maximum hardness and minimum polarizability by making use of two important aspects of DFT, viz., time-dependent (TD) DFT¹⁵ and excited-state DFT.¹⁶ To our knowledge, this is for the first time these electronic structure principles are studied in a dynamical system involving excited electronic states. It may, however, be noted that there is no general excited-state DFT¹⁷ but for some special cases such as in states which are of lowest energy for a given symmetry class¹⁸ or in an ensemble of states¹⁹ and these are the cases considered in the present work.

Because a system is generally more reactive in its excited state it is expected from the MHP and the MPP that a system would become softer and more polarizable on electronic excitation. This idea has been confirmed in the cases of atoms,²⁰ ions²⁰ and molecules²¹ for the lowest energy state of a particular symmetry and different complexions of a two-state ensemble.

In the present work, we study the time evolution of various reactivity parameters such as electronegativity, hardness and polarizability associated with a collision process between a proton and various helium isoelectronic systems ($X = \text{He}, \text{Li}^+, \text{Be}^{2+}, \text{B}^{3+}, \text{C}^{4+}$) in their ground and excited electronic states as well as in a two-state ensemble. This collision process may be considered to be a model mimicking the actual chemical reaction between an X atom and a proton to give rise to an $X\text{H}^+$ molecule as is the standard practice in chemical kinetics to visualize chemical reactions as collision processes.²² According to HSAB principle, *the proton, being a hard acid, is expected to prefer*

to bind those systems which are in their ground states where they are the hardest and the affinity of binding would keep on decreasing with electronic excitations or with an increase in the excited-state contribution in a two-state ensemble. Here, we verify this prognosis using TDDFT and excited-state DFT.

To test the efficacy of the present method on the reactivity behavior along a given group of the periodic table we also study the protonation of He, Ne, Ar, Kr, and Xe. The chemical reactions $\text{H}_2 + \text{H}^+ \rightarrow \text{H}_3^+$ and $\text{CO} + \text{H}^+ \rightarrow \text{HOC}^+ + \text{HCO}^+$ are also studied. For the former reaction H_2 is considered in both the ground and the excited states. The other reaction is chosen to specifically test the regioselectivity in the reaction involving a multiple-site molecule.

Computational Details

Dynamical profiles of various reactivity parameters associated with the collision process between a proton and several helium isoelectronic systems ($X = \text{He}, \text{Li}^+, \text{Be}^{2+}, \text{B}^{3+}, \text{C}^{4+}$) and their two-state ensembles are generated by solving a generalized nonlinear Schrödinger equation within a quantum fluid density functional framework^{23,24} for the TD charge and current densities required for the calculation of any reactivity index in a given instant. Various functionals used for this purpose and the numerical details are available elsewhere.²⁴ This procedure stems from the TDDFT.^{1,5,7} This initial boundary value problem has been solved by a leap-frog type finite difference scheme.²⁴ Initial ($t = 0$) near Hartree–Fock wave functions in ¹S, ¹P, ¹D, and ¹F electronic states for different helium isoelectronic systems are taken from Clementi and Roetti²⁵ and Mukherjee et al.²⁶ for the ground and excited electronic states, respectively. In case of the two-state ensemble the density is chosen as

$$\rho_{\text{ensemble}} = (1 - \omega)\rho_{\text{gs}} + \omega\rho_{\text{es}} \quad (5)$$

where ρ_{gs} and ρ_{es} are ground state²⁵ and excited state²⁶ (¹P, 1s2p configuration) densities, respectively, and ω is a real number^{19,27} that measures the relative weights of various electronic states present in the ensemble.

While the near Hartree–Fock ground-state wave functions of He, Ne, Ar, Kr, Xe are taken from Clementi and Roetti,²⁵ the 4-31G double-Zeta ground states of H_2 and CO as well as the excited state of H_2 are taken from Snyder and Basch.²⁸ Owing to the cylindrical symmetry of the diatomics, we have used cylindrical polar coordinates ($\bar{\rho}, \phi, z$) in our calculations. The internuclear axis is taken along the z direction and the $\bar{\rho} - z$ plane as the molecular plane. Because of the cylindrical symmetry all local quantities are evaluated at the ($\bar{\rho} - z$) points.

Electronegativity is calculated by extending Gordy's work²⁹ to a TD situation. The TD chemical potential becomes equal to the total electrostatic potential^{10,24} at a point r_μ , i.e.

$$-\chi(t) = \mu(t) = \int \frac{\rho(r,t)}{|r_\mu - r|} dr - \frac{Z_1}{|R_1 - r_\mu|} - \frac{Z_2}{|R_2 - r_\mu|} \quad (6)$$

where r_μ is the point at which the sum of functional derivatives of the total kinetic and exchange–correlation energies vanishes at that time step. This process is a TD extension of the method proposed by Politzer

- (13) (a) Berkowitz, M.; Ghosh, S. K.; Parr, R. G. *J. Am. Chem. Soc.* **1985**, *107*, 6811. (b) Ghosh, S. K.; Berkowitz, M. *J. Chem. Phys.* **1985**, *83*, 2976.
 (14) Parr, R. G.; Yang, W. *J. Am. Chem. Soc.* **1984**, *106*, 2976.
 (15) (a) Runge, E.; Gross, E. K. U. *Phys. Rev. Lett.* **1984**, *52*, 997. (b) Dhara, A. K.; Ghosh, S. K. *Phys. Rev. A* **1987**, *35*, 442.
 (16) Singh, R.; Deb, B. M. *Phys. Rep.* **1999**, *311*, 47.
 (17) Kohn, W., Private discussion.
 (18) (a) Gunnarson, O.; Lundqvist, B. I. *Phys. Rev. B* **1976**, *13*, 4274. (b) Ziegler, T.; Rauk, A.; Baerends, E. J. *Theor. Chim. Acta* **1977**, *43*, 261. (c) von Barth, U. *Phys. Rev. A* **1979**, *20*, 1693.
 (19) (a) Theophilou, A. *J. Phys. C* **1979**, *12*, 5419. (b) Hadjisavvas, N.; Theophilou, A. *Phys. Rev. A* **1985**, *32*, 720. (c) Kohn, W. *Phys. Rev. A* **1986**, *34*, 5419. (d) Gross, E. K. U.; Oliveira, L. N.; Kohn, W. *Phys. Rev. A* **1988**, *37*, 2805–2809. (e) Oliveira, L. N.; Gross, E. K. U.; Kohn, W. *Phys. Rev. A* **1988**, *37*, 2821.
 (20) Chattaraj, P. K.; Poddar, A. *J. Phys. Chem. A* **1998**, *102*, 9944; Chattaraj, P. K.; Poddar, A. *J. Phys. Chem. A* **1999**, *103*, 1274.
 (21) (a) Chattaraj, P. K.; Poddar, A. *J. Phys. Chem. A* **1999**, *103*, 8691. (b) Fuentealba, P.; Simon-Manso, Y.; Chattaraj, P. K. *J. Phys. Chem. A* **2000**, *122*, 348.
 (22) Laidler, K. J. *Chemical Kinetics*; Harper and Row: New York, 1987, Chapter 4.

- (23) Deb, B. M.; Chattaraj, P. K. *Phys. Rev. A* **1989**, *39*, 1696.
 (24) Chattaraj, P. K.; Sengupta, S. *J. Phys. Chem. A* **1997**, *101*, 7893.
 (25) Clementi, E.; Roetti, C. *At. Data Nucl. Data Tables* **1974**, *14*, 174.
 (26) Mukherjee, P. K.; Sengupta, S.; Mukherjee, A. *Int. J. Quantum Chem.* **1970**, *4*, 139.
 (27) (a) Nagy, A. *Phys. Rev. A* **1990**, *42*, 4388; Nagy, A. *Phys. Rev. A* **1994**, *49*, 3074. (b) Levy, M. *Phys. Rev. A* **1995**, *52*, 4313. (c) Chattaraj, P. K.; Ghosh, S. K.; Liu, S.; Parr, R. G. *Int. J. Quantum Chem.* **1996**, *60*, 535.
 (28) Snyder, L. C.; Basch, H. *Molecular Wave Functions and Properties: Tabulated From SCF Calculations In A Gaussian Basis Set*; John Wiley & Sons: New York, 1972; pp T-2 to T-3 and pp T-40 to T-41.
 (29) Gordy, W. *Phys. Rev.* **1964**, *69*, 604.

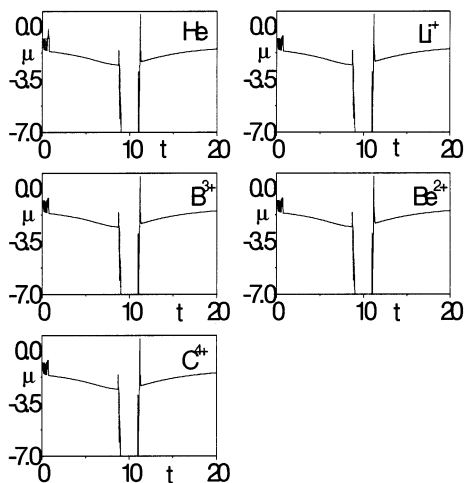


Figure 1. Time evolution of chemical potential (μ , au) during a collision process between an X-atom/ion ($X = \text{He}, \text{Li}^+, \text{Be}^{2+}, \text{B}^{3+}, \text{C}^{4+}$) in its ground state and a proton.

et al.³⁰ to calculate the covalent radii of atoms using electronegativity equalization principle.³¹ This definition of the TD chemical potential is akin to the functional derivative of a TD energy quantity.³² Electronic chemical potential has also been calculated using free energy density functionals in recent years which helps in ab initio molecular dynamics simulations within a grand canonical ensemble.³³ In eq 6, R_1 , R_2 , and Z_1 , Z_2 are radius vectors and atomic numbers of the target (X-atom/ion) and the projectile (H^+) nuclei, respectively. The origin of the coordinate system is fixed on the target nucleus and the position of the projectile is determined by a Coulomb trajectory.³⁴ A linear trajectory provides qualitatively similar results.³⁵

While TD hardness is calculated from eq 3, the TD polarizability is calculated as follows

$$\alpha(t) = |D_{\text{ind}}^Z(t)|/|G_Z(t)| \quad (7)$$

where $D_{\text{ind}}^Z(t)$ is the electronic part of the induced dipole moment and $G_Z(t)$ is the component of the external Coulomb field along the Z-axis mimicking the weak electric field generally used in defining the dynamic polarizability.

Results and Discussion

Ground and Excited States Reactivity Dynamics of Protonation of He-Isoelectronic Systems. Figure 1 depicts the time evolution of chemical potential associated with the collision process between a proton and an X-atom/ion ($X \equiv \text{He}, \text{Li}^+, \text{Be}^{2+}, \text{B}^{3+}, \text{C}^{4+}$) in its ground-state mimicking the corresponding chemical reaction.

Three distinct zones are discernible for the whole collision process: approach, encounter and departure. Neither r_μ nor μ is calculable in the encounter regime because the condition mentioned above is not satisfied anywhere in space. After the initial transients die out, μ becomes more or less stable in the approach regime. Toward the end of this regime and the beginning of the departure regime, μ changes drastically due

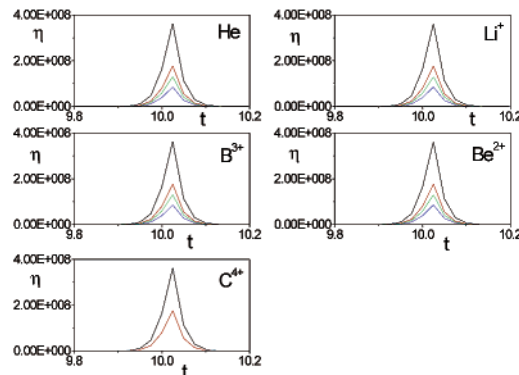


Figure 2. Time evolution of hardness (η , au) during a collision process between an X-atom/ion ($X = \text{He}, \text{Li}^+, \text{Be}^{2+}, \text{B}^{3+}, \text{C}^{4+}$) in various electronic states ($^1\text{S}, ^1\text{P}, ^1\text{D}, ^1\text{F}$) and a proton. (black line) ^1S ; (red line) ^1P ; (green line) ^1D ; (blue line) ^1F .

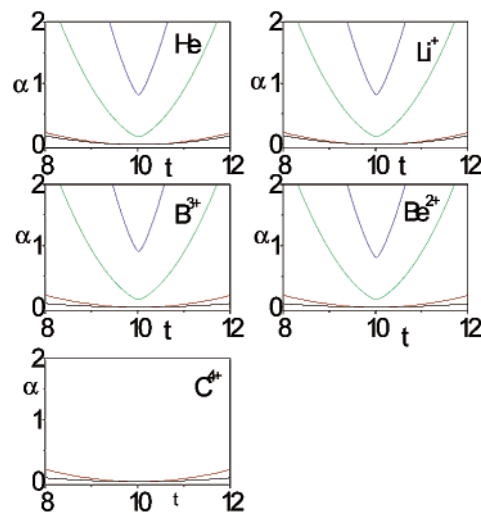


Figure 3. Time evolution of polarizability (α , au) during a collision process between an X-atom/ion and a proton. See the caption of Figure 2 for details.

to rapid charge oscillations. These time steps bracket the encounter regime where the electron density is shared by both the nuclei. In the departure regime, μ again changes drastically to reach a stable value more or less the same as that obtained in the approach regime. Because the qualitative features of the dynamic μ -profiles for the excited states and two-state ensembles are quite similar we refrain from presenting them here.

Dynamic profiles of η and α for the ground (^1S) and various excited states ($^1\text{P}, ^1\text{D}, ^1\text{F}$; for C, only ^1S and ^1P densities are available) of He isoelectronic atom/ions colliding with a proton are presented in Figures 2 and 3, respectively. In all cases, hardness gets maximized and polarizability gets minimized in the encounter regime signifying a favorable dynamical process vis a vis the dynamical variants of the MHP and MPP. Very large hardness and small polarizability values stem from the fact that the electron density is shared by both the nuclei in the encounter regime unlike the isolated atom/ion case where the electron distribution is spherical due to the central nature of the Coulomb potential originating from a single nucleus. It is known^{20,21} that any system becomes softer and more polarizable with electronic excitation i.e., for any given species $\eta_{^1\text{S}} > \eta_{^1\text{P}} > \eta_{^1\text{D}} > \eta_{^1\text{F}}$ and $\alpha_{^1\text{S}} < \alpha_{^1\text{P}} < \alpha_{^1\text{D}} < \alpha_{^1\text{F}}$ vindicating the MHP and MPP. Now, proton being a hard acid would prefer to bind with X ($X \equiv \text{He}, \text{Li}^+, \text{Be}^{2+}, \text{B}^{3+}, \text{C}^{4+}$) in the order $^1\text{S} > ^1\text{P} > ^1\text{D} > ^1\text{F}$, and hence, the maximum η value would decrease and the minimum α value

- (30) Polizer, P.; Parr, R. G.; Murphy, D. R. *J. Chem. Phys.* **1983**, *79*, 3859.
 (31) Sanderson, R. T. *Science* **1951**, *114*, 670. Sanderson, R. T. *Science* **1955**, *121*, 207. Sanderson, R. T. *J. Chem. Educ.* **1954**, *34*, 238.
 (32) Bartolotti, L. *J. Phys. Rev. A* **1982**, *26*, 2243. Deb, B. M.; Ghosh, S. K. *J. Chem. Phys.* **1982**, *31*, 238.
 (33) Vuilleumier, R.; Sprik, M.; Alavi, A. *J. Mol. Struct. (THEOCHEM)*, **2000**, *506*, 343; Tavernelli, I.; Vuilleumier, R.; Sprik, M. *Phys. Rev. Lett.* **2002**, *88*, 213 002–1;
 (34) Kulander, K. C.; Sandhya Devi, K. R.; Koonin, S. E. *Phys. Rev. A* **1982**, *25*, 2968.
 (35) Chattaraj, P. K.; Maiti, B., unpublished work.

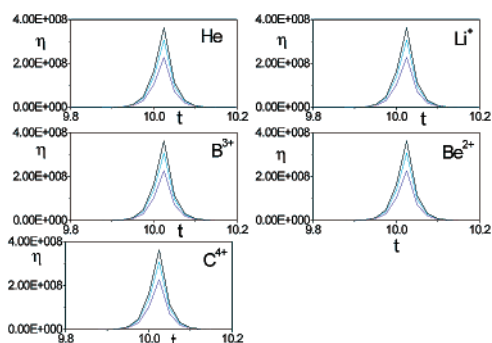


Figure 4. Time evolution of hardness (η , au) during a collision process between an X - atom/ion (X = He, Li⁺, Be²⁺, B³⁺, C⁴⁺) in different complexions of a two - state ensemble ($\omega = 0, 0.25, 0.5$) and a proton. (black line) $\omega = 0$; (cyan line) $\omega = 0.25$; (violet line) $\omega = 0.5$.

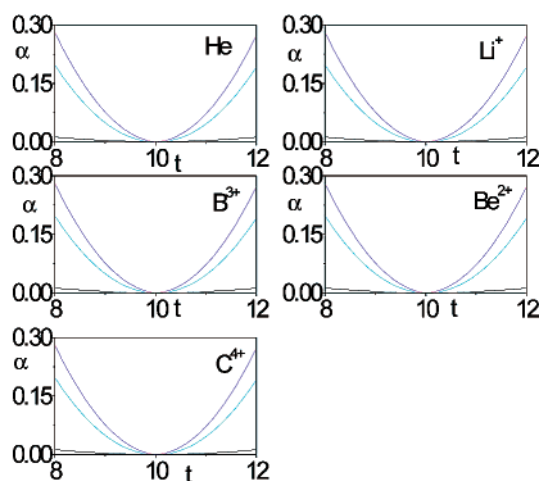


Figure 5. Time evolution of polarizability (α , au) during a collision process between an X-atom/ion and a proton. See the caption of Figure 4 for details.

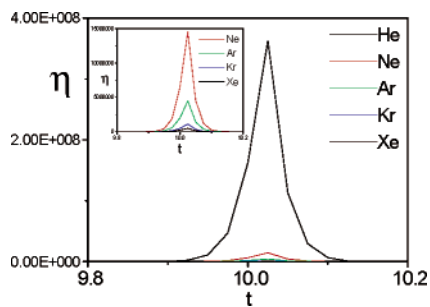


Figure 6. Time variation of hardness (η , au) of He, Ne, Ar, Kr, Xe during protonation.

would increase in the order ${}^1S \rightarrow {}^1P \rightarrow {}^1D \rightarrow {}^1F$, which is precisely the case providing the validity of the HSAB principle in a dynamical context.

Figures 4 and 5 depict respectively the time dependence of η and α for various complexions of a two-state ensemble ($\omega = 0, 0.25$ and 0.5) of X (X = He, Li⁺, Be²⁺, B³⁺, C⁴⁺) colliding with a proton. In the encounter regime η maximizes and α minimizes in all cases as would have been predicted by the MHP and the MPP for a favorable chemical reaction. As expected from a dynamical variant of the HSAB principle vis a vis the validity of the MHP and the MPP the maximum η value decreases and the minimum α value increases with an increase in the excited-state contribution in a two-state ensemble.

Reactivity Dynamics of Protonation of Noble Gas Systems.

Figures 6 and 7, respectively, depict the time variation of

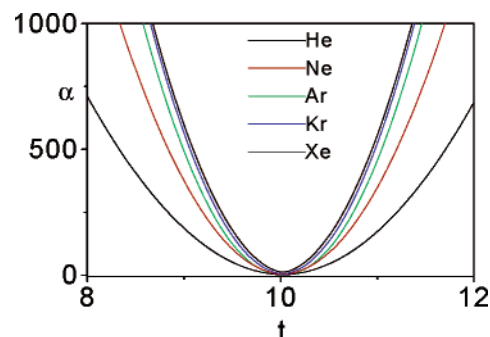


Figure 7. Time variation of polarizability (α , au) of He, Ne, Ar, Kr, Xe during protonation.

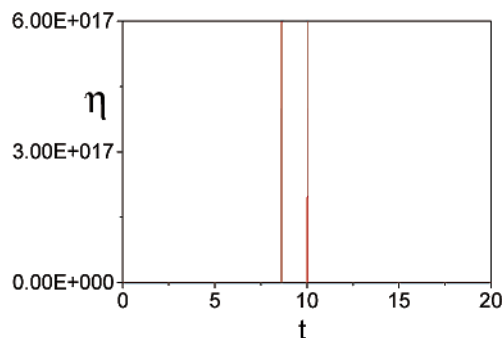
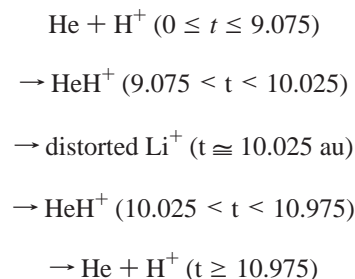


Figure 8. Time evolution of hardness (η , au) during a collision process between a hydrogen molecule in its ground state and a proton.

hardness and polarizability of He, Ne, Ar, Kr, Xe during protonation. The actual chemical reaction may be envisaged as follows



Hardness attains a maximum value and polarizability attains a minimum value in the encounter regime, as expected. The hardness maximum decreases and the polarizability minimum increases as we proceed in the sequence He \rightarrow Ne \rightarrow Ar \rightarrow Kr \rightarrow Xe. It is a clear-cut signature of increasing reactivity in that sequence corroborating the fact that Xe is the most reactive according to the MHP and MPP which has been the reason behind the fact that the first attempt of compound formation of noble gas elements was tried on Xe.

Dynamic Reactivity Profiles of the Chemical Reaction: $\text{H}_2 + \text{H}^+ \rightarrow \text{H}_3^+$. The density profile of the H₂ molecule in its ground (${}^1\Sigma_g^+$) state is symmetric at both nuclei (See figure provided in the Supporting Information). It is expected that during protonation the hardness would get maximized and the polarizability would get minimized in the neighborhood of the nuclei since the density attains its maximum values at those points and they would be symmetric which is what precisely obtained in the present work. The hardness profile is depicted in Figure 8 and the polarizability profile is provided in the Supporting Information. We also calculate the corresponding

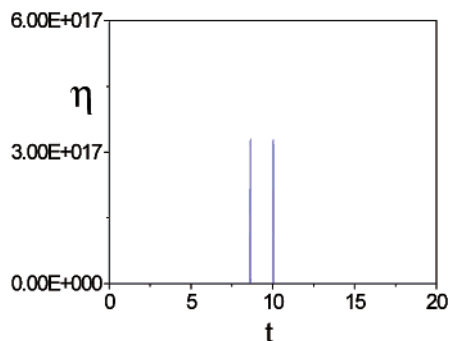


Figure 9. Time evolution of hardness (η , au) during a collision process between a hydrogen molecule in its first excited state and a proton.

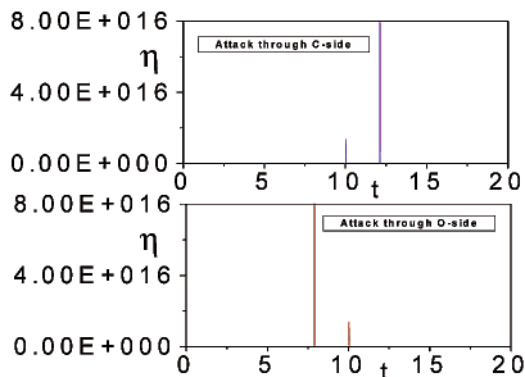


Figure 10. Dynamic hardness (η , au) profile for protonation of CO considering the attack from both the carbon and oxygen sides.

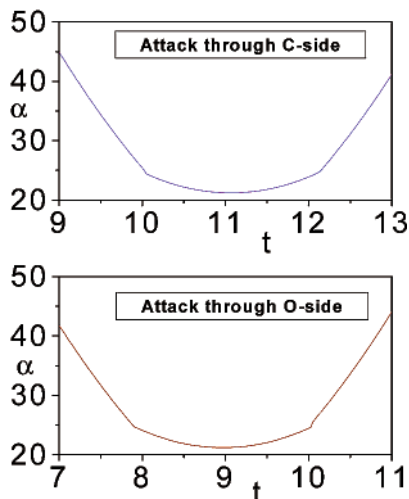


Figure 11. Dynamic polarizability (α , au) profile for protonation of CO considering the attack from both the carbon and oxygen sides.

profiles for the first excited state of H_2 . As in the ground state, the hardness profile is presented in Figure 9, whereas supporting material contains the polarizability plot. Being softer and more polarizable this state exhibits lower η_{\max} and higher α_{\min} values when compared to the corresponding values for the ground state.

Regioselectivity of the Chemical Reaction. $CO + H^+ \rightarrow HCO^+ + HOC^+$. The density profile of CO in its ground state is presented in the Supporting Information. Electron density is centered around the C and O nuclei with the latter having larger contribution as also discerned²⁸ by the corresponding Mulliken charges of respectively 5.7991 and 8.2009. Figures 10 and 11 respectively depict the dynamical hardness and polarizability profiles for protonation considering the attack from both the

carbon and oxygen sides which are consistent. According to these figures, vis a vis the MHP and MPP the O-site is kinetically more favored for protonation. This explains the laboratory synthesis³⁶ of isoformyl cation HOC^+ as well as its presence in the dense interstellar cloud³⁷ such as in the source Sagittarius B2. Proton being a hard acid would prefer to attack at the harder O-end. It may be noted that in the formation of metal carbonyls CO often attacks through the softer C-site to the soft metal atoms in their low oxidation states. Moreover, when CO acts as an electrophile, attack is predominantly via the C-site (due to the low energy π^* LUMO with high amplitude on the carbon atom), and hence, the O-site has relatively more nucleophilic character and accordingly larger affinity toward H^+ . Condensed local softness of C is much larger than that of O in CO as has been revealed by both ab initio SCF and DFT calculations.³⁸ Formation of HOC^+ is thus suggested by both HSAB principle as well as Klopman's theory³⁹ of charge-controlled hard-hard interactions. Once HOC^+ is formed it may rearrange itself to go over to the thermodynamically more stable⁴⁰ formyl cation HCO^+ .

Thus, the HSAB principle manifests itself in a dynamical context as well. Now, chemical processes can be understood and analyzed better, from start to finish, with the help of HSAB principle.

Concluding Remarks

To understand the dynamical behavior of chemical reactivity indices during a chemical reaction involving ground and excited electronic states, a model collision process between an X-atom/ion ($X \equiv He, Li^+, Be^{2+}, B^{3+}, C^{4+}$) and a proton is studied within a quantum fluid density functional framework. The whole collision process can be divided into three distinct regimes, viz., approach, encounter and departure in terms of the time-dependent electronegativity profile. In the encounter regime where the actual chemical process takes place, hardness maximizes and polarizability minimizes as expected from the principles of maximum hardness and minimum polarizability. A system becomes softer and more polarizable with electronic excitation as well as where the excited-state contribution in a two-state ensemble increases. The maximum hardness value decreases and the minimum polarizability value increases in the encounter regime for these situations. Because proton is a hard acid this fact is a *clear-cut signature of the HSAB principle in a dynamical situation*.

Reactivity of noble gas elements toward protonation increases in the sequence $He \rightarrow Ne \rightarrow Ar \rightarrow Kr \rightarrow Xe$. In the reaction: $H_2 + H^+ \rightarrow H_3^+$ hardness maximizes and polarizability minimizes in the neighborhood of the two nuclei. Excited-state H_2 is more reactive than the ground-state H_2 . Regioselectivity of protonation is toward the O-end of CO which in turn can reorganize to HCO^+ .

Acknowledgment. We are grateful to Professor W. Kohn for helpful discussions and CSIR, New Delhi for financial as-

- (36) Gudeman, S. C.; Woods, R. C. *Phys. Rev. Lett.* **1982**, *48*, 1344.
 (37) Woods, R. C.; Gudeman, S. C.; Dickman, R. L.; Goldsmith, P. F.; Huguenin, G. R.; Irvine, W. M.; Hjalmarson, A.; Nyman, L. A.; Olofsson, H. *Astrophys. J.* **1983**, *270*, 583.
 (38) Oláh, J.; Alsenoy, C. V.; Sannigrahi, A. B. *J. Phys. Chem. A* **2002**, *106*, 3885.
 (39) Klopman, G. *J. Am. Chem. Soc.* **1968**, *90*, 223; Chattaraj, P. K. *J. Phys. Chem. A* **2002**, *105*, 511.
 (40) Dixon, D. A.; Komornicki, A.; Kraemer, W. P. *J. Chem. Phys.* **1984**, *81*, 3603.

sistance. We would like to thank the anonymous reviewers and Professor Donald G. Truhlar, Associate Editor of *J. Am. Chem. Soc.* for very constructive criticisms.

Supporting Information Available: Figure showing the electron density of the H₂ molecule in its ground ($^1\Sigma_g^+$) state,

symmetric at both nuclei, the polarizability profiles in the ground and the first excited states, and the density profile of CO in its ground state. This material is available free of charge via the Internet at <http://pubs.acs.org>.

JA0276063